Accepted Manuscript

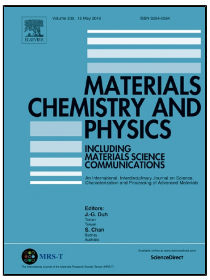

Size Control Synthesis of Pure Ni nanoparticles and Anodic-Oxidation of Butan-1-ol in Alkali.

Senjuti Banik, Ankita Mahajan, Swapan kumar Bhattacharya

PII:	S0254-0584(19)30539-5
DOI:	10.1016/j.matchemphys.2019.121747
Article Number:	121747
Reference:	MAC 121747
To appear in:	*Materials Chemistry and Physics*
Received Date:	04 September 2018
Accepted Date:	12 June 2019

Please cite this article as: Senjuti Banik, Ankita Mahajan, Swapan kumar Bhattacharya, Size Control Synthesis of Pure Ni nanoparticles and Anodic-Oxidation of Butan-1-ol in Alkali., *Materials Chemistry and Physics* (2019), doi: 10.1016/j.matchemphys.2019.121747

Size Control Synthesis of Pure Ni nanoparticles and Anodic-Oxidation of Butan-1-ol in Alkali.

Senjuti Banik, Ankita Mahajan, Swapan kumar Bhattacharya*

Physical Chemistry Section, Department of Chemistry,

Jadavpur University, Kolkata – 700 032, India.

***Email – skbhatt7@yahoo.co.in,**

Tel.: +919831699643, Fax: +913324146584

Abstract

Different sets of nickel nanoparticles with confined average diameter in the range: 9.4 - 13.7 nm are synthesized by varying different parameters of wet chemical method to investigate the effects of such parameters on anode catalysis in oxidation of butan-1-ol in aqueous alkali. The structure and morphology of the synthesized nanoparticles and the role of Ni and its oxides as catalyst in the oxidation of butan-1-ol have been characterized by X-ray diffractometry, scanning and transmission electron microscopy, infrared spectroscopy, cyclic voltammetry and chronoamperometry. The average particle diameter of each set is controlled by the duration of heating of precursor solution of different compositions. The required heating time and the attained maximum temperature of the reaction mixture change by changing the amount of reducing agent, solvent composition and pH of the solution. In alkali, graphite supported Ni nanoparticles form $Ni(OH)_2$ and then on application of potential NiOOH which is electro-catalytically active towards the oxidation of butan-1-ol. The catalytic activity of the as synthesized material is found to depend on the diameter of the nanoparticles, purity of the synthesized Ni nanoparticles and molecular environment around catalyst which in turn depends on the production parameters. The study reveals greater catalytic activity and increased ratio of carbonate to butanoate in the products using the pure nano-catalyst obtained by the least time of heating.

Keywords

Pure Ni nanoparticles, Butanol oxidation, electrocatalysis, study of products

1. Introduction

Electrochemical oxidation of small organic compounds like aliphatic and aromatic primary alcohols has great importance in both research [1-3] and industry [4]. It is useful in a variety of fields like energy storage, organic synthesis, fuel cells, waste water treatment, sensors, medical and environmental analyses. Although few methods for electro oxidation of alcohol to corresponding acids have been reported [5], there exist many problems like cost, yield, selectivity, stability, adulteration etc, which need investigation and address.

A large number of metals (Pt, Au, Ru, Co, Ni, Cu, etc) and oxides or hydroxides are extensively studied as electrochemical catalysts [6, 8]. Among all the metals Ni is suitable for numerous applications because of higher natural abundance, lower cost and lower toxicity. Many Ni based materials including Ni^{+2}, Ni, NiO, $Ni(OH)_2$ and NiOOH have been reported [9-12], which exhibit excellent electro-catalytic activity toward the oxidation of small organic compounds such as methanol, ethanol, glucose, cyclohexanol, ammonia, urea etc [13, 6]. Apart from these, surface adhered Ni^{+2}/Ni^{+3} redox couples have also been used in electrosynthetic works and for sensing of alcohols and sugars. Among oxidation of different types of alcohols, significant number of studies has been dedicated to methanol and ethanol but only a few to propanol [14, 15] and, very few studies are available for butanol [16, 17] despite the latter can be obtained from natural resources and different substances. Moreover, butanol is less volatile, less toxic and obtained from natural sources, and possesses relatively high flash point of 35^0C which is important for safety reason. In the study, Butan-1-ol is investigated because it is the most active isomer among all the C_4–alcohols [18] and expected to show good performance like C_3–alcohols [15]. The reactions of partial and complete anodic oxidations of butan-1-ol are given by equation (1) and (2).

$$CH_3CH_2CH_2CH_2OH + 5\ OH^- = CH_3CH_2CH_2COO^- + 4\ H_2O + 4e^- \quad (1)$$

$$\text{And } CH_3CH_2CH_2CH_2OH + 32\ OH^- = 4\ CO_3^{2-} + 21\ H_2O + 24\ e^- \quad (2)$$

So, it can be told from the corresponding Nernst equations that the electrode potential would be reduced at high pH making the oxidation process favourable. Other advantages in using alkali as the medium are less poisoning, easy formation of metal to metal hydroxide which is either main or co-catalyst and, wider possibility of using materials as catalysts, etc. So the kinetics of alcohol oxidation can be improved significantly in alkali [19, 20]. Pt and Pd are the 'state of the art' catalysts for alcohol oxidation. Despite Ni occupies the same group of the periodic table and much cheaper, it is only tested in relatively few cases. On the other hand, Ni can easily form hydroxide and oxy-hydroxide layers when immersed in alkali [21]. It also form mono hydroxide at lower potential than these required for Pt and Pd [22]. In recent years, Ni and Ni-based materials are found to have attractive activity toward the electro-oxidation of some organic and inorganic molecules like ethanol, methanol, ammonia, hydrazine hydrate and urea due to their superb catalytic activity, high ductility, good thermal conductivity, low cost, high strength, and fair electrical conductivity. Ni materials have received enormous attention due to their distinctive properties in magnetic, thermal, electrical and chemical fields. It has been proved to have tremendous capability as electrode materials in batteries, super capacitors, additives in oil, magnetic carriers for biomedical and others [23-26].

Many techniques have been used for the synthesis of Ni nanoparticles including micro-emulsion [27, 28], solvothermal reduction [29], polyol process [30-32], microwave [33], sonochemical [34], gas phase condensation [35] and thermal decomposition of organic complexes [36-39]. Polyol method is one of the efficient methods used in the past two decades by using poly-alcohol as both solvent and reducing agent [40]. The poly-alcohol can be either ethylene glycol (EG), diethylene glycol or 1, 2-propanediol. It is also suggested that EG may be adsorbed to the surface of particles to prevent undesired surface oxidation [41]. Another crucial part in the synthesis of Ni nanoparticles is their tendency to aggregate with

each other because of their magnetic behaviour. Under certain environment Ni nanoparticles tend to form secondary particles which are the results of van der Waals attractive forces, magnetic dipole interactions and thermodynamic driving force [42, 43]. This paper describes a facile and rapid synthesis of pure Ni nanoparticles by modified polyol method using N_2H_4 as a reducing agent and NaOH for maintaining optimum pH. Our focus was to reduce the temperature of the synthesis by changing the constituents of the reaction mixture and to observe the effect of such changes to control the average diameter and the change in catalytic property of the synthesized particles in reference to oxidation of butanol in alkali. The formation of nanoparticles was confirmed using X-ray diffraction (XRD) and different microscopic techniques. The catalytic capability of each set of nanoparticles dispersed on a graphite substrate was compared in reference to the oxidation of butan-1-ol in alkali and promising better kinetic result was obtained with pure Ni nanoparticles synthesized by exerting the least time of heating.

2. Experimental

2.1. Chemicals

All chemicals were purchased from Merck (India) and used without further purification. Milli-Q water was used to make all solutions. All the glass apparatus were properly cleaned with chromic acid and then rinsed with Millipore water.

2.2. Synthesis of Ni Nano-Particles

The nickel nanoparticles were synthesized using polyol method [44] by reduction of Ni^{+2} in an aqueous solution with hydrazine hydrate. Detailed experimental conditions used in the syntheses are given in Table 1. In a typical synthetic procedure, 5 mL of 0.1 M solution of $NiCl_2.6H_2O$ (clear green colour) was mixed with 3 mL of pure ethylene glycol by gentle stirring. This was followed by addition of hydrazine monohydrate in a single act under well

stirring condition of the mixture to form blue Ni-hydrazine complexes. After addition of hydrazine to the green nickel chloride solution, the solution turned into blue colour. The solution changed to turbid blue violet colour after continuous stirring. Appropriate amount of 0.5M NaOH was then mixed to maintain the pH of the solution to 12-13. Then the solution was heated under strong magnetic stirring in a hot oil bath until the colour of the solution changed suddenly to black which indicated the formation of Ni nanoparticles. Then the heating was stopped, the solution was kept at the bath for ten minutes and finally cooled to room temperature. The time required for the sudden change of colour and the temperature of the solution raised at the moment are presented in Table 1.

Table 1 Experimental parameters describing different environments and condition of synthesis of four sets of Ni nanoparticles having diameters confined within 9.4 nm-13.7 nm

Synthesis parameter set numbers	Compositions of reaction mixture and other synthesis parameters							Average size of crystallites obtained from XRD (nm)	Catalyst synthesised
	Metal Precursor (5 mL) (M)	Hydrazine monohydrate (mL)	0.5 M NaOH (mL)	Ethylene glycol (mL)	Water added (mL)	Temperature (^{0}C) when colour changes occur	Heating time (min) when colour changes occur		
1.	0.1	0.5	1.5	3	10	100ºC	120	9.4	Ni(1)
2.	0.1	0.5	1.5	10	3	80ºC	60	9.4	Ni(2)
3.	0.1	0.5	3	10	1.5	70ºC	30	13.7	Ni(3)
4	0.1	2	3	10	0	60ºC	15	10.1	Ni(4)

The black precipitate obtained was separated by centrifugation and washing with water for several times and then dried in vacuum desiccators to collect as powder. The stoichiometric equation of the reaction can be expressed as:

$2Ni^{2+} + N_2H_4 + 4OH^- = 2Ni + N_2 + 4H_2O$.

For synthesis of four different sets of Ni nanoparticles (Ni (1-4)), the amount of reducing agent (hydrazine) and the capping agent cum co-solvent (EG) are changed according to that presented in Table 1, with an aim to reduce the duration of heating and the maximum temperature of the reaction mixture, without much varying the average global diameter of the synthesized nanoparticles.

2.3. Structural characterization

Powder X-ray diffraction (XRD) study of the synthesised Ni nano-particles was carried out using X-ray diffractometer (XRD, Philips 1710, USA) with CuKα radiation (λ= 1.541 Å). X-ray photoelectron spectroscopy (XPS) was done using XPS, Omicron, serial no 0571. The surface morphology and the microstructures of all the synthesised catalysts were investigated with a JEOL JSM-6700F Field Emission Scanning Electron Microscope (FE-SEM). Shape and size of the nano-particles were investigated using high resolution transmission electron microscope (HRTEM) (JEM-2100 HRTEM, JEOL, Japan). Ex-situ Fourier transform infra-red study was carried out for semi solid products using perkin Elmer instrument (Spectrum RX1, resolution $4cm^{-1}$).

2.4. Electrochemical measurements

All electrochemical measurements were carried out at 27 $\pm$ 2°C in a two compartment glass cell fitted with a three electrode assembly by using a computer aided Potentiostat/Galvanostat (AEW-2, Muniststst, Sycopel Scientific Ltd, UK). The flat end surface of the graphite rod (geometrical surface area 0.24 cm^2) in which synthesised catalysts were deposited by typical drop casting technique [45] was used as working electrode and a Pt foil (1 cm $\times$ 1 cm) and $Hg/HgO/OH^-$ (0 1M) electrode (MMO) having equilibrium electrode potential 0.1 V with respect to standard hydrogen electrode (SHE) were used as counter and reference electrode respectively. Cyclic voltammetry (CV) and chronoamperometry (CA) were carried out in 0.1

M NaOH solution with and without butanol of strength 0.1 M. All cyclic voltammograms were recorded after steady profiles were obtained.

2.5. Studies of the products

Following our previous studies [45, 46], a current density of 30μA cm^{-2} is drawn from 0.1M butanol in 0.1M NaOH solution in N_2 atmosphere for 72h using constructed electrodes like Ni(1)/C, Ni(4)/C as anodes in separate experiments and a large Pt electrode is used as cathode in each case. Resulting solution was dried in vacuum and the obtained semi solid product was used in ex-situ FTIR study using FTIR spectrophotometer (Perkin Elmer, SN-74514, Spectrum RX1, having resolution 4 cm^{-1}). High performance liquid chromatography (HPLC) (Shimadzu Corporation, Japan) of products of butanol oxidation was executed by using the solution left after drawing current at 0.5 V with respect to MMO for 2h.

3. Results and discussion

Nickel nanoparticles were synthesized from a nickel hydrazine mixture in a sodium hydroxide environment at high pH (12-13) which is favourable to form nickel nanoparticles [47, 48]. Figure 1 shows the changes of colour of the solution during the stepwise progress of the reaction. The pale green colour of Ni-EG complex changed to blue due to formation of $[Ni(N_2H_4)_2]^{2+}$ which in turn forms violet coloured complex $[Ni(N_2H_4)_3]^{2+}$ on heating and stirring. On further addition of NaOH solution, it turns black due to formation of Ni nanoparticles by reduction as evident from Fig. 1a-1d.

The complexing and reducing agent, hydrazine (N_2H_4) has a standard reduction potential of −1.16V in an alkaline solution, for the reaction: $N_2 + 4H_2O + 4e^- = N_2H_4 + 4OH^-$ [47]. Nickel ion, which has a standard reduction potential of −0.25V, is consequently reduced by hydrazine following equation: $2Ni^{2+} + 4e^- = 2Ni$. Therefore, a chemical reduction process of the nickel ion with hydrazine as reducing agent occurs in an alkaline aqueous solution according to the following equation: $2Ni^{2+} + N_2H_4 + 4OH^- \rightarrow 2Ni + N_2 + 4H_2O$. Solution pH

influences the synthesis of the nickel nanoparticles as can be seen from the Nernst equation (3).

$$E = E^0 - \frac{RT}{4F}\ln\frac{1}{[OH^-]^4[Ni^{2+}]^2}$$

$$= E^0 + \frac{2.303\,RT}{4F}\log\{[OH^-]^4[Ni^{2+}]^2\} \quad (3)$$

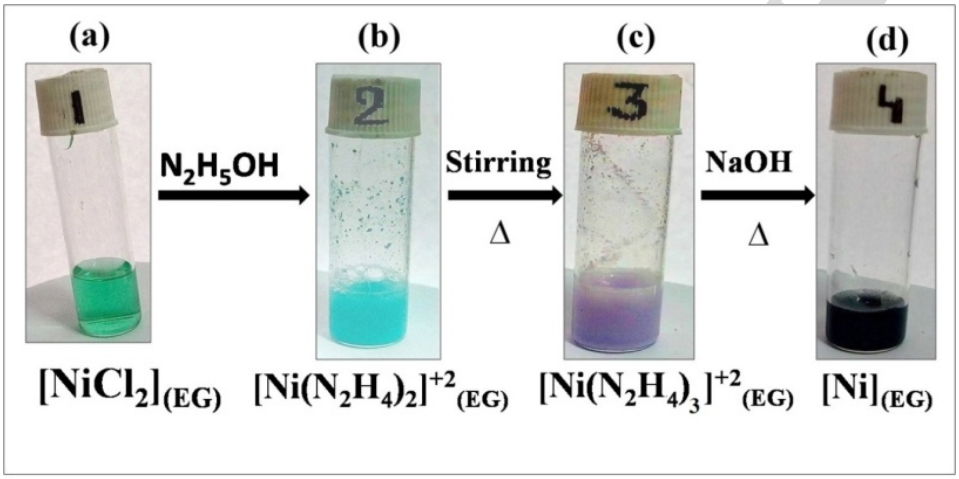

Fig. 1 Colour changes of the solution at the different stages of synthesis during reduction of Ni^{+2} to Ni.

The increased concentration of OH^- i.e., high pH is therefore favourable for such reaction. But higher pH also facilitates precipitation of metal hydroxide. This is because the standard reduction potential of $Ni(OH)_2$ is −0.72V for the reaction: $Ni(OH)_2 + 2e^- = Ni + 2OH^-$.So, in order to avoid precipitation of hydroxide, an optimum pH range of 12-13 is maintained in the study.

3.1. Tuning of Ni nanoparticles

Four sets of Nickel nanoparticle of almost similar crystallite diameter (9.4-13.7 nm) have been synthesized by varying at least two of the following reaction parameters like slight variation of pH, cosolvent (EG) composition, amount of reducing agent (NH_2-NH_2) and the

duration of heating. In Ni (2), the crystallite size is controlled by increasing the content of EG in aqueous reaction mixture causing decrease in time of heating with respect to that used for preparation of Ni (1). EG may act as an internal heat reservoir instigating similar crystallite size. In Ni (3), the heating time is more reduced by increasing the solution pH with respect to that used for preparation of Ni (2). The increased pH of the reaction mixture helps reduction of Ni^{+2} but OH^- ion also takes up several water molecules for its solvation affecting less number of water molecules left for solvation /stabilization of synthesized nano particles. As a result of the two opposing factors, the net effect is only slight increase in the average size of crystallites of synthesized Ni nanoparticles marked as Ni (3) with respect to that marked as Ni (2). To synthesize Ni (4), the time of heating is still decreased (15 minute) by increasing the amount of the reducing agent, hydrazine mono hydrate by four times, keeping all other synthesis parameters same with respect to that used for synthesis of Ni (3). The result is the crystallites of the synthesized nanoparticle having diameter of 10.1 nm which is very near to 9.4 nm as that obtained for the first two samples. Notably, the temperature of the observed starting of colour change which was also the maximum temperature of the reaction mixture (Table. 1) decreased gradually from Ni (1) to Ni (4) with increase of other favourable parameters like increased concentration of EG, OH^- , hydrazine in the synthesis. Thus one can successfully synthesize Ni nano particles of almost same crystallite size by suitably adjusting different reaction parameters.

3.2. Size and morphology of synthesized nanoparticles

XRD measurement was conducted to obtain the crystallographic information of the prepared nanoparticles. The broadened peaks at 44.56º, 51.84º and 76.21º in the Fig. 2 assign for diffraction from the planes (111), (200) and (220) respectively of a face centred cubic (fcc) phase of pure Ni nanoparticles as reported in JCPDS, (ICDD) 2003 file numbered 897128. The sharp diffraction peaks are found for all synthesized nanoparticles having diameter

between 9.4 and 13.7 nm as calculated from Debye-Scherrer's equation (Table 2). For sample Ni(1-3) an additional peak arises at 59.7º for (117) plane of orthorhombic primitive nickel oxide hydroxide (Ni_2O_2OH) as reported in JCPDS, (ICDD) 2003 file numbered 841459. This compound is electrochemically inactive [49] and not produced at lower temperature.

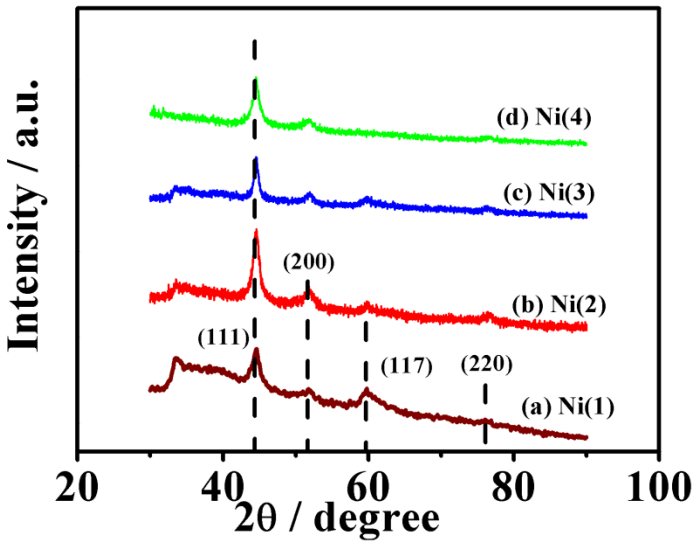

Fig. 2 XRD patterns of the synthesized Ni (1-4) nanoparticles.

In fact, the relative intensities of this peak of Ni_2O_2OH as obtained with respect to peak of (111) plane of Ni for different samples follow the order: Ni(4) [0] < Ni(3) [0.43] < Ni(2) [0.45] < Ni(1) [0.76], indicating that the production of Ni_2O_2OH increases with increase of temperature (vide Table 1). Moreover, Ni(4) which has been synthesized using the least time of heating, does not contain any Ni_2O_2OH.

Table 2 Diffraction peaks, crystallite size, and lattice parameter of synthesized nanoparticles

Nanoparticles	Position of 2θ (degree)	d spacing from XRD (Å)	Calculated d spacing (Å)	Crystallite size (nm) from XRD	Cell Parameter (Å)
Ni(1)	44.56	2.03	2.02	9.4	3.51
	51.84	1.76	1.75		
Ni(2)	44.56	2.03	2.02	9.4	3.51
	51.77	1.76	1.75		
Ni(3)	44.56	2.03	2.02	13.7	3.51
	51.73	1.76	1.75		
Ni(4)	44.56	2.03	2.02	10.1	3.51
	51.77	1.76	1.75		

The chemical states of the synthesized Ni nanoparticles have been studied further by XPS analysis and the spectra are shown in Fig. 3. The XPS survey spectra of Ni (1) and Ni (4) samples (Fig. 3a) exhibit the peaks corresponding to binding energies at about 286.2 and 530 eV which are assigned to C1s and O1s orbital, respectively. The peaks in the marked portions in Fig. 3a represent the binding energies of Ni 2s, 2p and 3p orbital without any other impurity. Peak for C is originated from the carbon tape employed for XPS studies. The ratio of peak areas of Ni2p and O1s is 1:8.31 for Ni(1) sample, whereas the same ratio for Ni(4) sample is 1:6.73. This signifies surface of Ni(1) is relatively more oxidized than that of Ni(4) samples. Fig. 3b reveals that a small peak corresponding to binding energy 852.21 eV for metallic Ni appears for Ni(4) sample besides the two major peaks centred at 855.27 and 873.13 eV corresponding to Ni 2p3/2 and Ni 2p1/2 and their satellite peaks at a binding energy of 861.04 eV and 879.36 eV respectively. Notably, the peak for metallic Ni is negligibly small/absent in the profile (Fig. 3c) for Ni(1) sample indicating complete oxidation of metallic Ni at the surface of the sample. These evidences indicate that Ni(1) is more susceptible to oxidation than Ni(4). This in turn indirectly supports the formation of Ni_2O_2OH as an added product in Ni(1) unlike Ni(4) sample.

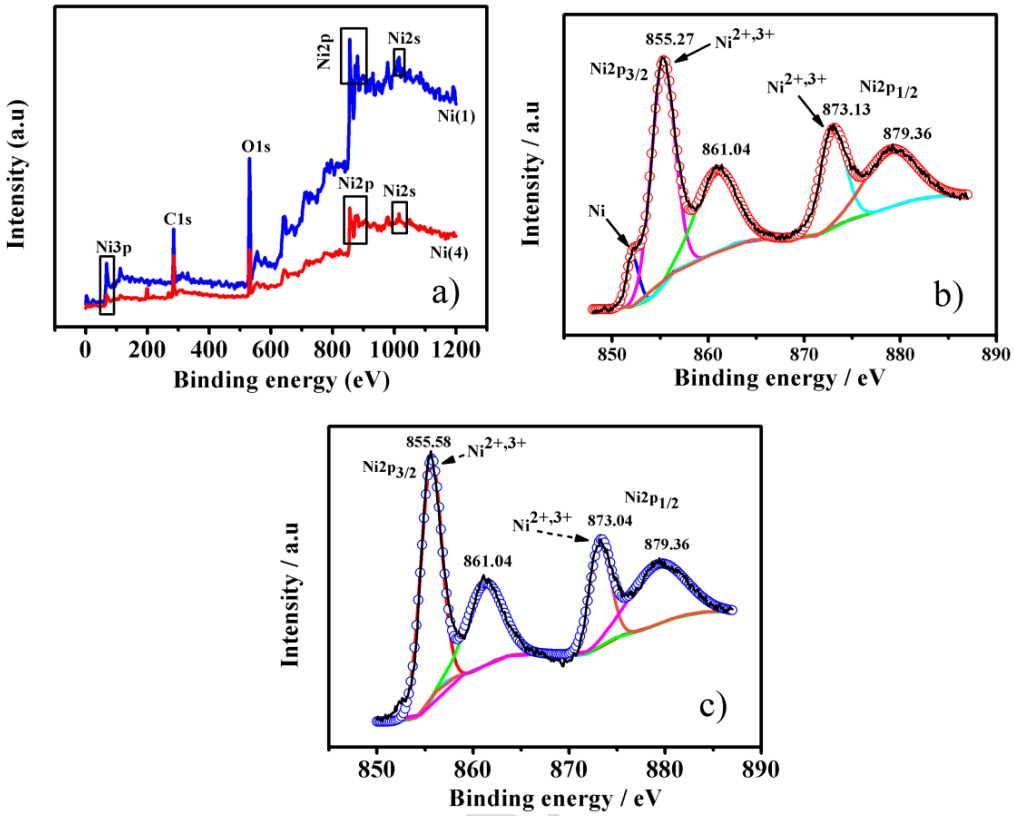

Fig. 3 The XPS spectra of Ni nanoparticles (a) Survey spectrum (b) Ni 2p of Ni(4) (c) Ni 2p of Ni(1)

To understand the morphology of the electrode surface, analyses of FE-SEM images as presented in Fig. 4 are performed. Fig. 4a reveals the spherical granules in the partial agglomerated state for Ni(1) sample. In Fig. 4b, spherical particles are agglomerated to form compact flake structure. These structures of Fig. 4a and 4b are relatively compact with less holes. In Ni(3), as evident in Fig. 4c, agglomerated nanoparticles form layer structures like that of Ni(2) but with increased black hole portion. Fig. 4d divulges that particles of Ni(4) sample in nm range are closely agglomerated with significant number of black holes giving rise increased penetrating sites for the reactants with the benifit in catalysis.

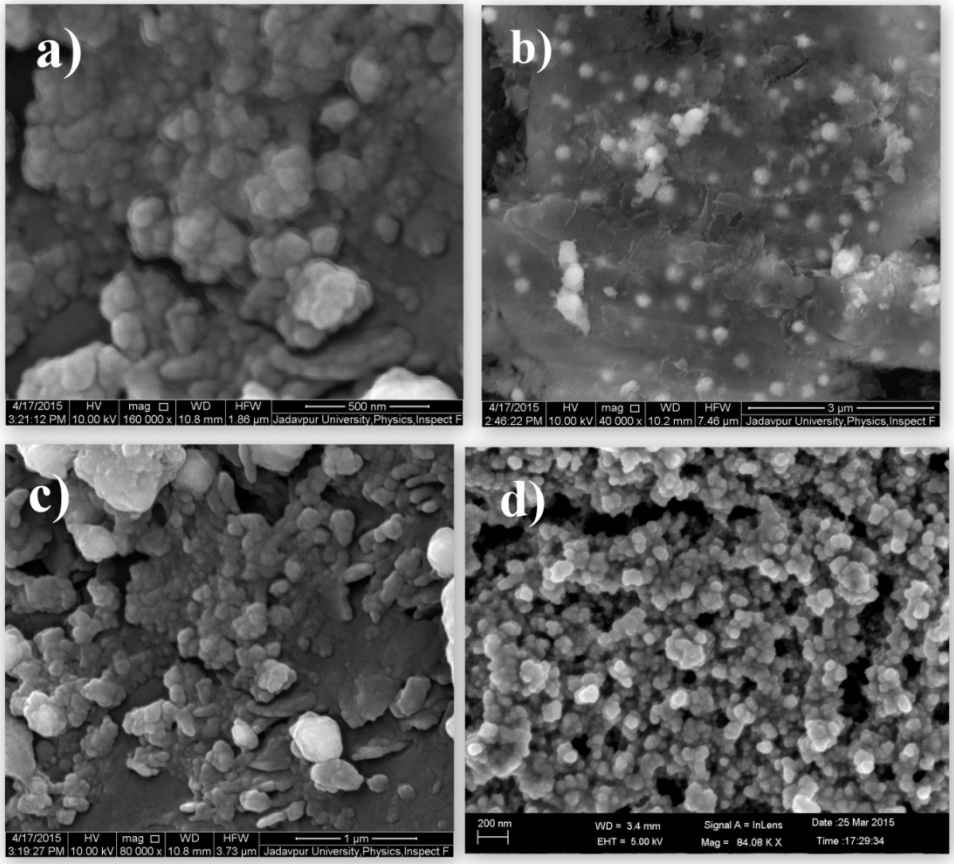

Fig. 4 FESEM images of (a) Ni(1), (b) Ni(2), (c) Ni(3) and (d) Ni(4).

The transmission electron microscope (TEM) and selected area electron diffraction (SAED) images further authenticate the microstructure of synthesized Ni nano-particles. Fig. 5a and 5b show the microstructure of Ni(4)and Ni(3) having values of diameters, ca. 14 nm and 24 nm respectively. Fig. 5a represent the HRTEM image of Ni(4), which shows clear lattice fringes with lattice spacing of 2.02 Å signifying the dominance of (111) plane. This is in good agreement with the XRD results that also explain that the ratio of intensity of (111) peak is much larger than that of others. A set of diffraction rings can be clearly seen in the corresponding SAED pattern of Ni(4) as presented in the inset of Fig. 5a. The SAED pattern

analysis reveals that the lattice spacing obtained from the first ring is 2.03 Å, which is well consistent with the data obtained from XRD measurements. In combination with the XRD results, the fringes can be indexed as (111) and the other rings as reflections from different planes of the face centered cubic (fcc) lattice of Ni(4).

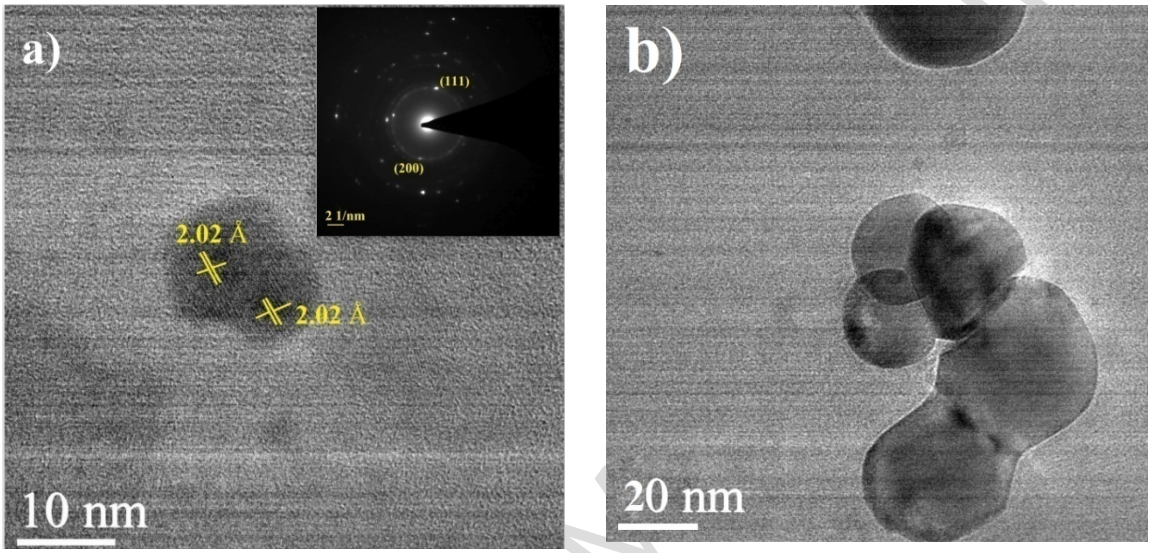

Fig. 5 TEM image of Ni (4) (a) Ni (3) (b). Inset of (a) presents SAED pattern of Ni (4)

3.3. Electrochemical studies

Electrocatalytic activity of graphite-supported nickel nanoparticles was done by cyclic voltammetry (CV) study in 0.1 M NaOH solution within a Potential range of -0.9V to +0.6V vs MMO at a scan rate 50 mV s^{-1}. Figure 6a shows that no peak appears for nafion coated graphite electrode indicating base materials are inactive in alkali throughout the potential range studied. It is well established [50, 52] that oxidation of Ni to $Ni(OH)_2$ in alkali gives a peak at around –0.5V just after hydrogen evolution reaction on Ni during anodic scan of potential in CV. Since it is not obtained here, it indicates that the surface of Ni nanoparticles is primarily covered by $Ni(OH)_2$ formed during exposition of the thin film electrode in air

and/or immersion in alkali for CV measurement. The corresponding reverse peak is also not found due to possible complexation of Ni^{2+} with oxidation products of ethylene glycol or destabilization of $NiOH^{+}$ as suggested by others [53-55]. The conversion of Ni^{+2} to Ni^{+3} [$Ni(OH)_2$/NiOOH] and vice versa occur according to the reaction (4) with a peak at ~0.51 V in anodic and at ~0.35 V in cathodic directions, as usual [56]

$$Ni(OH)_2 + OH^- \rightleftharpoons NiO(OH) + H_2O + e^- \quad (4)$$

In presence of butanol, NiOOH oxidises it, itself being reduced to $Ni(OH)_2$ by chemical reaction: $2NiOOH + C_4H_{10}O = C_4H_8O + 2Ni(OH)_2$ (5)

followed by $2NiOOH + C_4H_8O + OH^- = C_4H_7O_2^- + 2\ Ni(OH)_2$ (6)

and part or full of the complete electrochemical reaction:

$2NiOOH + C_4H_7O_2^{2-} + 25OH^- = 4CO_3^{2-} + 2\ Ni(OH)_2 + 15H_2O + 19\ e^-$ (7)

in various steps as presented in CV profiles of Fig. 6b

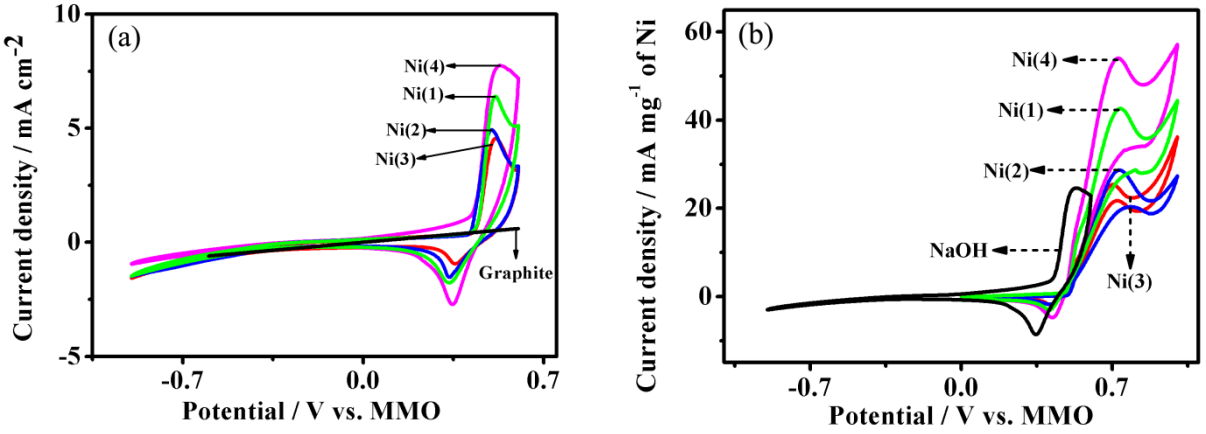

Fig. 6 Cyclic voltammograms of different Ni/C and bare graphite electrodes in (a) 0.1 M NaOH solution and (b) 0.1 M BuOH in 0.1 M NaOH solution at a scan rate of 50 mV s^{-1}.

Thus the peak current is increased in presence of butanol in comparison to that in blank NaOH in absence of butanol.

The cyclic voltammetric study of the different Ni electrodes has been performed for alkaline oxidation of butanol using different scan rates. The plots of anodic peak current density (forward scan) versus square root of scan rate ($v^{1/2}$) for different electrodes (Fig. 7a), reveal that the forward peak current densities are linearly varied with the square root of scan rate at the lower scan rates indicating that the butanol oxidation reaction on carbon supported Ni electrodes in alkaline media is initially a diffusion controlled process as also found in our earlier study [45, 46]. From these straight lines, the diffusion coefficients of OH^- is determined at the lower scan rates, using the relation

$$i_P = 2.72 \times 10^5 \, n^{3/2} \, D^{1/2} \, c^o \, v^{1/2} \qquad (8)$$

where D is in $cm^2 \, s^{-1}$, c^o in mole cm^{-3} and v in V s^{-1}. For different electrodes the order of 10^7 times diffusion co-efficient (presented within parenthesis) of OH^- ion in $cm^2 \, s^{-1}$on the surface of thin film is given by Ni(3) (0.032) < Ni(2) (0.042) < Ni(1) (2.24) < Ni(4) (9.80).

The low values of diffusion co-efficient signify the presence of protecting agent and also nafion membrane which prohibits the approach of reactant molecules toward the electrodes and limited active zones (molecules of $Ni(OH)_2$) at the surface for fruitful reaction following equation (4).

The straight line plot of E_F versus log v (Fig. 7b), helps determining the standard rate constant, Ks in cm s^{-1} of the reaction (1) from the slope and intercepts of the plot following equation (9)

$$E_F = E_{1/2} - b \left[0.52 - \log \frac{b^{\frac{1}{2}} K_s}{D^{1/2}}\right] - \frac{b}{2} \log v \qquad (9)$$

The half wave potential $E_{1/2}$ is given by using the relation

$$E_F = E_{1/2} - \frac{1.1RT}{nF} \qquad (10)$$

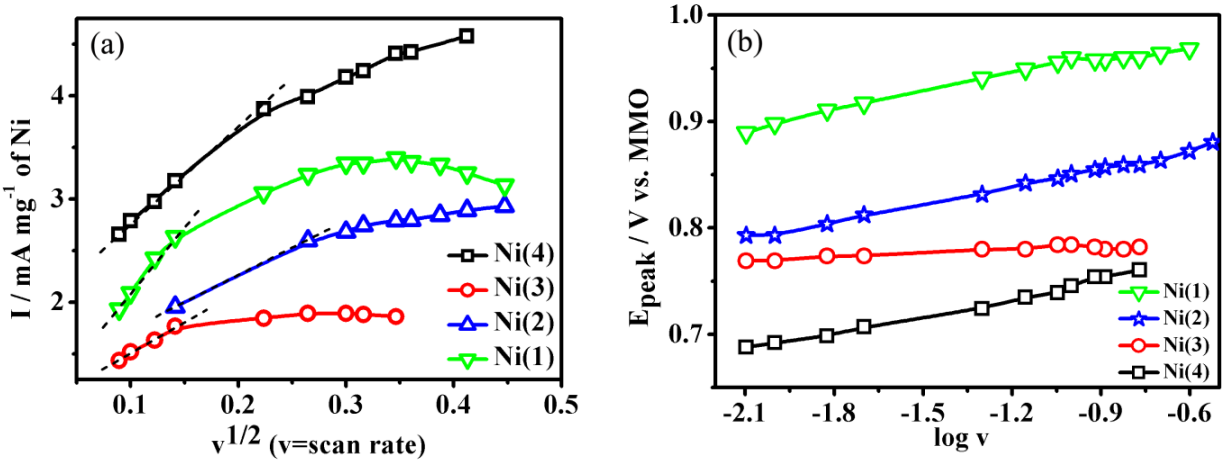

Fig. 7 (a) Plots of peak current density versus square root of scan rate and (b) Plots of peak potential versus log of scan rate for different Ni / C electrodes in 0.1 M BuOH in 0.1 M NaOH solution obtained from cyclic voltammetric studies at different scan rates.

Table 3 Cyclic voltammetric studies of synthesized nanoparticles for the oxidation of 0.1 M BuOH in 0.1 M NaOH solution at room temperature at a scan rate of 50 mV s^{-1}

Electrodes	Onset Potential/V	Loading/mg of Ni cm^{-2}	E_f/V	E_b/V	I_f/mA cm^{-2}	I_b/mA cm^{-2}	I_f'/mA of Ni	mg^{-1}
Ni(1)	0.492	0.2982	0.735	0.408	12.72	-0.9314	42.65	
Ni(2)	0.492	0.3284	0.733	0.408	9.42	-0.5937	28.68	
Ni(3)	0.489	0.3184	0.703	0.409	8.09	-0.588	25.40	
Ni(4)	0.482	0.3148	0.724	0.422	17.01	-1.4807	54.03	

The k_S found (represented in cm s^{-1} within the parenthesis) for different electrodes are in the orders Ni(4) (10.47×10^6) > Ni(3) (312.86) > Ni(2) (85.12) > Ni(1) (0.107). Moreover, the onset potentials of BOR on the electrodes follow the same order in reverse sequence: Ni(4) < Ni(3) < Ni(2) < Ni(1) as evidenced from Table 3.

These two experimental facts indicate the decreasing order of the apparent catalytic activity as guided by both the Gibbs energy of activation of the reaction using the synthesized materials and the relative amount of the purest state or the activity of the catalyst material present at the surface of the electrodes. The order reflects that the standard rate constant is increased as the inactive $Ni_2O_2(OH)$ is less or not produced with the synthesis of different sets of Ni nanoparticle. Notably, the average diameters of the sets of Ni nanoparticle are not much different (9.4 to 13.7 nm). So the effect of change of average diameter of the particles is very small in comparison to other effects like purity of the as synthesized samples. Greater the purity of the Ni catalyst, as revealed by the XRD studies, greater is the rate constant obtained in the different synthesis processes. The peak current densities, (I_f, I_f' and I_b) however follow the order Ni(4) > Ni(1) > Ni(2) > Ni(3), which indicates that not only the purest state but also the factor of surface area/diameter of the synthesized nanoparticles and molecular environment around the nanoparticle surface are important in influencing the overall rate of reaction. Notably, the I_f value for the electrode containing Ni(4) material is greater for reaction presented by equation (4), in alkali in presence of butanol in comparison to that in absence of it whereas the reverse peak current density I_b shows the opposite behaviour. This can be corroborated by the reduction of NiOOH by methods other than electrochemical one i.e. oxidation of butanol by NiOOH following reactions (5) and (6).

3.4. Potentiodynamic polarization (PDP) study

For comparing the kinetic activities of Ni / C electrodes towards BOR, Tafel polarization analysis of the catalysts were executed following linear Tafel relation according to

$$E = E_e - \frac{2.303RT}{\alpha F} log i_0 + \frac{2.303RT}{\alpha F} \log i \qquad (11)$$

Where the terms bear usual significance [17] and the parameters are provided in Table 4.

To calculate the exchange current density, equilibrium potential is set to 0.55 V versus. NHE, which represents the equilibrium potential of oxidation of Ni^{+2} to Ni^{+3}. Considering the potential shift of Hg/HgO in 0.1M NaOH (0.1638 V) the calculated E_{theory} becomes 0.3912 V. Tafel slopes were obtained from potentio-dynamic current measurements of 0.1M butanol in 0.1M NaOH solution in the potential range -0.9V to +0.6V at a scan rate of 2 mV s^{-1} (Fig. 8) like other [45].

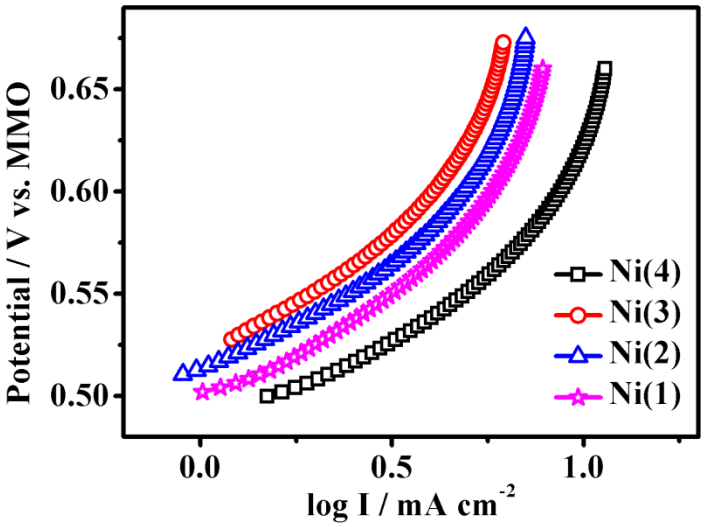

Fig. 8 Tafel plots for various Ni/C catalysts obtained from CV studies of 0.1 M BuOH in 0.1 M NaOH solution at a scan rate of 2 mV s^{-1}

Table 4 Data obtained from chronoamperometry, cyclic voltammetric study (scan rate 2 mV s^{-1}

Electrodes	Chronoamperometry at 0.5 V current density (mA mg^{-1} of Ni)	Tafel slope (V dec^{-1}) (scan rate 2 mV s^{-1})	Exchange current density, I_0 (mA cm^{-2})
Ni(1)	0.96	0.181	0.36
Ni(2)	0.85	0.180	0.28
Ni(3)	0.62	0.196	0.31
Ni(4)	1.25	0.181	0.55

The exchange current density obtained by extrapolating the linear fitted Tafel line to where over potential equals to zero. The results are presented in Table 4 which shows that the exchange current density of Ni / C electrodes varies in the order Ni(4) > Ni(1) > Ni(3) > Ni(2), revealing the overall catalytic activity in the near equilibrium region.

3.5. Chronoamperometric (CA) study

The relative catalytic activity and stability of the electrodes are also tested using chronoamperometry in a solution of 0.1 M butanol in 0.1 M NaOH with a fixed potential of 0.5 V (vs Hg/HgO) for 300s. Figure 9 illustrates the profiles which show that the catalytic activity as measured by the constant current densities (presented within the parenthesis in $mAmg^{-1}$ of Ni) of the electrodes varies in the order: Ni(3) (0.62)< Ni(2) (0.85) < Ni(1) (0.96)< Ni(4) (1.25), which is same as the peak current density values obtained from CVs. The initial rapid decrement in current density was observed due to double layer formation and generation of the reactive intermediates which block the surface during oxidation of butanol. Subsequently, the current decreases slowly and reached a pseudo steady state.

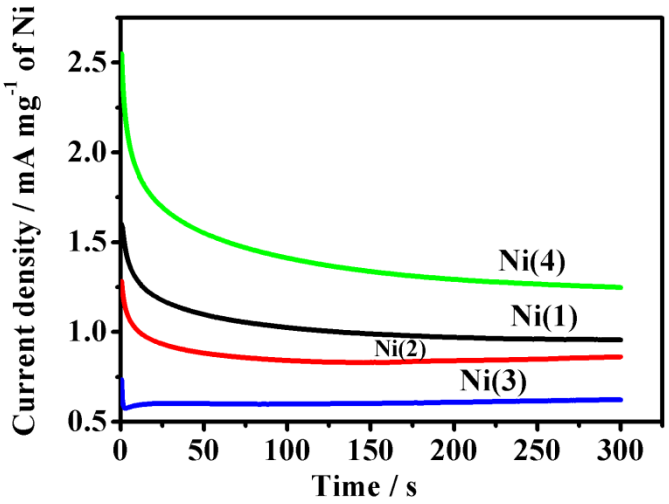

Fig.9 Chronoamperometric profiles for different Ni/C electrodes for 0.1 M BuOH in 0.1 M NaOH solution at a potential of 0.5 V up to 300 sec.

In all electrochemical measurements of CV, CA and PDP studies, the change in overall catalytic activity for the 4 sets of Ni nanoparticles is small due to similar crystallite size of these particles. However the change in catalytic capabilities of different sets of particles is definite because these are found to be the same from different studies (CV, CA, PDP). The electrocatalytic capability of particles of Ni(2) is less than that of Ni(1) is seemingly due to the greater presence of adsorbed EG around Ni nanoparticles, which opposes the butanol molecules to approach to the Ni catalyst. The electrocatalytic capability of particles of Ni(3) is lower than that of Ni(2), because of lower particle size of Ni(2) than that of Ni(3). The electrocatalytic property of Ni(4) is the best among all the sample. This is possibly because of the fact that only this sample contains greater amount of pure Ni nanoparticles at the surface of the electrodes. In all other samples electro-inactive Ni_2O_2OH is formed in association with Ni nanoparticles. For this the current density obtained with this sample is the largest.

Table 5 reveals that the peak current per unit geometrical area, i.e. peak current density of the presently synthesized Ni electrodes are much better than that of the bulk Pt and Pd electrodes found in the literature. The best electrode (Ni(4)) found in the study shows 2.3 and 13.9 times more peak current density with respect to bulk Pd and Pt for BOR at a scan rate of 50 mV s^{-1} at 25°C. Therefore, considering cost effectiveness of Ni, in comparison to noble metals, the present electrodes and particularly that made with Ni(4) can be recommended for effective anodes for butanol fuel cell.

Table 5 Literature review of Butanol oxidation on various catalysts immersed in 0.1M butanol in 0.1M NaOH at 25° C and at 50 mV s^{-1}.

Electro-catalyst	Current density (mA cm^{-2})	References
Pt	0.4	[48]

Au	3.4	[48]
Pd	0.5	[48]
Pd (bulk)	7.31	[10]
Pt (bulk)	1.22	[10]
Ni(4) (nano)	17.01	This paper

3.6. Study of the products

Main FTIR bands observed for the products of butanol oxidation in alkaline medium are presented in Table 6. Figure 10 and Table 6 reveal that the peak (P_3) at ca 872 cm^{-1}, that arises due to CO_3^{2-} ions, is less sharp for Ni(1) than that of Ni(4) electrode. For each electrode, the most intense broad peak (P_2) appears at ca 1468 cm^{-1} due to both carbonate and butanoate ions. There are weak peaks at ca 1763 $cm^{-1}$and 1759 cm^{-1} for Ni(4) and Ni(1) electrodes respectively, which indicate the presence of aldehyde (-CHO) group and confirms that oxidation of butanol occurs through the formation of butanal as intermediate. Moreover the ratio of absorbance corresponding to (P_3) and (P_1) is much greater for Ni(4) (1.14) than Ni(1) (1.02). It indicates formation of both butanoate and carbonate and that the formation of carbonate is relatively greater for Ni(4) through C-C bond breaking of butanol. Since the peaks for carbonate are found among the products of BOR, the CV studies of possible intermediates of BOR like butanal and butanoate are thought to be beneficial.

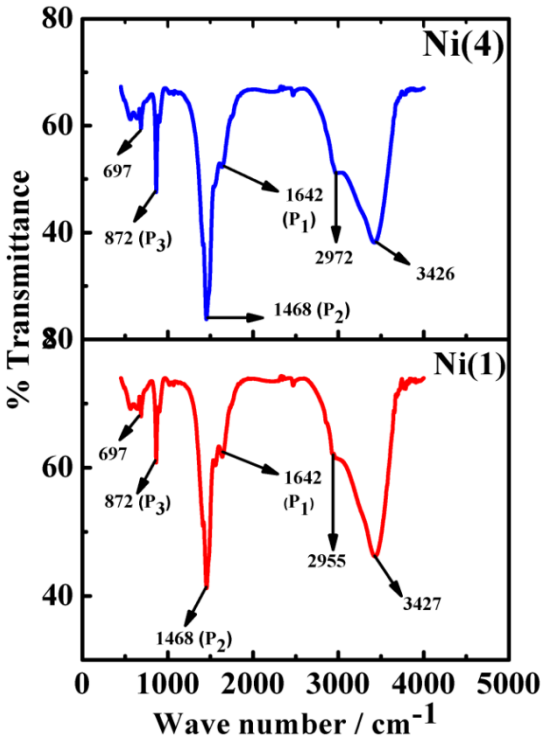

Fig. 10 Ex-situ FTIR profiles of the products of BOR for Ni/C (1) and Ni/C (4) catalysts.

Table 6 Assignments of main FTIR bands observed from spectra of the products of butanol oxidation in alkaline medium.

Sample-1		Sample-4	
Wave number (cm^{-1})	Possible assignments	Wave number (cm^{-1})	Possible assignments
2955	-CH symmetrical stretching	2972	-CH symmetrical stretching
1759	Carbonyl (C=O) stretching	1763	Carbonyl (C=O) stretching
1642	butanoate	1642	butanoate
1468	butanoate/carbonate	1468	Butanoate/carbonate
872	carbonate	872	carbonate
697	carbonate	697	carbonate

HPLC study of the solution after BOR on the electrodes constructed with Ni(1) (solution 1) and Ni(4) samples (solution 2), reveals the formation of at least 4 compounds marked, as evident from the 4 peaks depicted in Fig. 11. The compounds produced are sodium butyrate (10.65), butyraldehyde (5.69), sodium carbonate (6.59), and butyl butyrate (3.03) for both the electrodes. It is evident from the peak areas that all the compounds are produced more with electrodes constructed with Ni(4) than that with Ni(1) which indicates Ni(4) is better catalyst than Ni(1). The ratio of the peak areas for butyrate: carbonate: butyraldehyde : butyl butyrate is 1:1.97:3.68:24.62 on Ni(4) electrodes. The same ratio for Ni(1) electrode is 1:1.57:2.14:10.70. This indicates that the formations of butyraldehyde and butyl butyrate are facilitated on Ni(4) based electrode in conformation with the results of electrochemical studies.

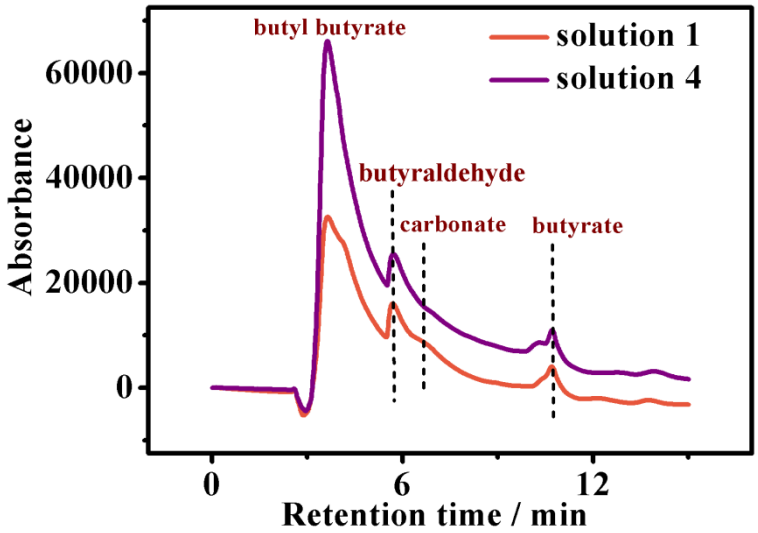

Fig. 11 HPLC study of the product solutions of butanol on Ni(1) and Ni(4) samples

Figure 12 illustrates the CV profiles of NaOH (0.1M) without any fuel (blank) or in presence of 18mM of either of the fuels butanol, butanal, butanoate. The blank profile shows a single peak at 0.52 V due to reaction (1).

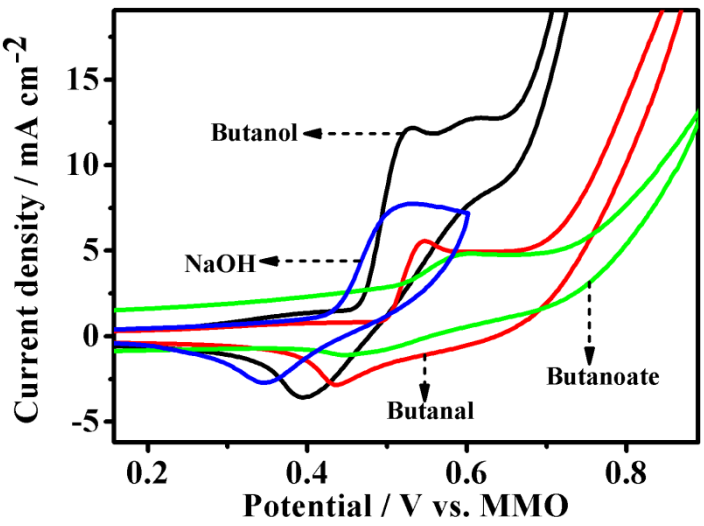

Fig. 12 Cyclic voltammograms (CVs) on nano Ni on Butanol, Butanal, Butanoate each at concentration of 18mM in 0.1 M NaOH solution.

In presence of butanol, butanal and butanoate, the corresponding peaks are shifted to 0.529 V, 0.546 V, and 0.595 V respectively. This indicates that the initial oxidation of butanol (by NiOOH) is easier than oxidation of butanal which on turn is easier than oxidation of butanoate. In case of oxidation of butanol two peaks are formed, among which the last peak appears at almost the same potential (0.607 V) as that of pure butanoate. Moreover, the related portion of CV of oxidation of butanol is almost similar in nature to that for pure butanal and butanoate, despite the current values are less. The greater surface coverage and low kinetics of the latter molecules than these of methanol are seemingly responsible for the

lower peak current values It appears that oxidation of butanol becomes difficult as it progresses through butanal and butanoate

4. Conclusion

Ni nanoparticles of almost same average diameter of crystallites (9.4-13.7 nm) can be successfully synthesized by simultaneous change of reaction parameters including the lowering of reaction temperature and duration of heating. It is found that the Ni nanoparticles synthesized by using the least time (15 minutes) of heating, for which a maximum temperature of the reaction mixture (4) is reached to 60^0 C, is obtained in the purest form which is also the best catalyst among all the synthesized nanoparticles in reference to the electrochemical oxidation of butanol in alkali. Formation of electrochemically inactive nickel oxide hydroxide at higher temperatures observed during syntheses might be the cause of lower current density with the other catalysts. The peak current density obtained with the drop-coated synthesized Ni nanoparticle in CV study of BOR reveals that it is at least 14 and 2.3 times greater than that with bulk Pt and Pd electrodes respectively. The electrode constructed with Ni(4) can also oxidise butanal and butanoate in addition to butanol .Since FTIR and HPLC studies support the formation of butyl butanoate, butanal, sodium butanoate and sodium carbonate, the electrode seems to be capable of oxidising butanol to carbonate at least to a little extent. The steady state chronoamperometric and equilibrium exchange current density obtained with the synthesized catalysts are found to be enough high for use of these anode-materials in cost-effective butanol oxidation in alkali. The study also signifies that the simultaneous change of reaction parameters may be effective to control the average diameter of the synthesized particles. Moreover, the purity and the catalytic activity of such Ni nanoparticles with confined diameter, synthesized from different molecular environment, are quite different.

Acknowledgements

We the authors gratefully acknowledge Jadavpur University and DST India, for financial assistance.

References

[1] Z.X. Liang, T.S. Zhao, J.B. Xu, L.D. Zhu, Mechanism study of the ethanol oxidation reaction on palladium in alkaline media, Electrochimica Acta 54 (2009) 2203-2208.

[2] A. Heinzel, V.M. Barragan, A review of the state-of-the-art of the methanol crossover in direct methanol fuel cells, J. Power Sources 84 (1999) 70-74.

[3] J. Bagchi, S. K. Bhattacharya, The effect of composition of Ni-supported Pt-Ru binary anode catalysts on ethanol oxidation for fuel cells, J. Power Sources 163 (2007) 661-670.

[4] R. Dillion, S. Srinivasan, A.S. Arico, V. Antonucci, International activities in DMFC R&D: status of technologies and potential applications, J. Power Sources 127 (2004) 112-126.

[5] R. L. Augestine, 'oxidation', Vol 1, Marcel Decker, New York (1969) p. 56.

[6] V. Vedharathinam, G.G. Botte, Understanding the electro-catalytic oxidation mechanism of urea on nickel electrodes in alkaline medium, Electrochim. Acta 81 (2012) 292-300.

[7] P.S. Roy, S.K. Bhattacharya, Size-controlled synthesis, characterization and electrocatalytic behaviors of polymer-protected nickel nanoparticles: a comparison with respect to two polymers, RSC Advances 4 (2014) 13892-13900.

[8] S. Das, K. Dutta, P.P. Kundu, Sulfonated polypyrrole matrix induced enhanced efficiency of Ni nanocatalyst for application as an anode material for DMFCs, Mater. Chem. Phy.176 (2016) 143-151.

[9] J.B. Raoof, A. Omrani, R. Ojani, F. Monfared, Poly(N-methylaniline)/nickel modified carbon paste electrode as an efficient and cheep electrode for electrocatalytic oxidation of formaldehyde in alkaline medium, J. Electroanal. Chem. 633 (2009) 153-158.

[10] I. Danaee, M. Jafarian, A. Mirzapoor, F. Gobal, M.G. Mahjani, Electrooxidation of methanol on NiMn alloy modified graphite electrode, Electrochim. Acta 55 (2010) 2093-2100.

[11] D. Wang, W. Yan, G.G. Botte, Exfoliated nickel hydroxide nanosheets for urea electrolysis, Electrochem. Commun. 13 (2011) 1135-1138.

[12] L.A. Hutton, M. Vidotti, A.N. Patel, M.E. Newton, P.R. Unwin, J.V. Macpherson, Electrodeposition of nickel hydroxide nanoparticles on boron-doped diamond electrodes for oxidative electrocatalysis, J. Phys. Chem. C 115 (2010) 1649-1658.

[13] M. Jafarian, M.G. Mahjani, H. Heli, F. Gobal, M. Heydarpoor, Electrocatalytic oxidation of methane at nickel hydroxide modified nickel electrode in alkaline solution, Electrochem. Commun. 5 (2003) 184-188.

[14] J. Ye, J. Liu, C. Xu, S.P. Jiang, Y. Tong, Electro-oxidation of 2-propanol on Pt, Pd and Au in alkaline medium, Electrochemcommun. 9 (2007) 2760-2763.

[15] J. Liu, J. Ye, C. Xu, S.P. Jiang, Y. Tong, Electro-oxidation of methanol, 1-propanol and 2-propanol on Pt and Pd in alkaline medium, J. Power Sources 177 (2008) 67-70.

[16] D. Takky, B. Beden, J.M. Leger, C. Lamy, Evidence for the effect of molecular structure on the electrochemical reactivity of alcohols: part III. Electro-oxidation of the butanol isomers on platinum single crystals in an alkaline medium, J. Electroanal. Chem. 256 (1988) 127-136.

[17] P. Mukherjee, S.K. Bhattacharya, Anodic oxidation of butan-1-ol on Pd and Pt electrodes in alkaline medium, J. Appl. Electrochem. 44 (2014) 857-866.

[18] D. Takky, B. Beden, J.M. Leger, C. Lamy, Evidence for the effect of molecular structure on the electrochemical reactivity of alcohols: part III. Electro-oxidation of the butanol isomers on platinum single crystals in an alkaline medium, J. Electroanal. Chem. 256 (1988) 127-136.

[19] C.W. Xu, P.K. Shen, Electrochemical oxidation of ethanol on Pt–CeO_2/C catalysts, J. Power Sources 142 (2005) 27-29.

[20] A.V. Tripkovic, K.D. Popovic, J.D. Lovic, V.M. Jovanovic, A. Kowal, Methanol oxidation at platinum electrodes in alkaline solution: comparison between supported catalysts and model systems, J. Electroanal. Chem. 572 (2004) 119-128.

[21] Y. Miao, L. Ouyang, S. Zhou, L. Xu, Z. Yang, M. Xiao, R. Ouyang, Electrocatalysis and electroanalysis of nickel, its oxides, hydroxides and oxyhydroxides toward small molecules, Biosens. Bioelectron. 53 (2014) 428-439.

[22] J. Bagchi, S.K. Bhattacharya, Electrocatalytic activity of binary Palladium Ruthenium anode catalyst on Ni-support for ethanol alkaline fuel cells, Trans Met chem. (2007) 32-47.

[23] D. Chen, J. Li, C. Shi, X. Du, N. Zhao, J. Sheng, S. Liu, Properties of Core-Shell Ni-Au Nanoparticles Synthesized through a Redox-Transmetalation Method in Reverse Micro-emulsion, Chem. Mater. 19 (2007) 3399-3405.

[24] X. Wu, W. Xing, L. Zhang, S. Zhuo, J. Zhou, G. Wang, S. Qiao, Nickel nanoparticles prepared by hydrazine hydrate reduction and their application in supercapacitor, Power Technology 224 (2012) 162-167.

[25] S. Qiu, Z. Zhou, J. Dong, G. Chen, J. Tribol, Preparation of Ni Nanoparticles and evaluation of their tribological performance as potential additives in oils 123 (2001) 441-443.

[26] T. Hyeon, Chemical synthesis of magnetic nanoparticles, ChemCommun. 21 (2003) 927-934.

[27] J. Ahmed, S. Sharma, K.V. Ramanujachary, S.E. Lofland, A.K. Ganguli, Microemulsion-mediated synthesis of cobalt(pure fcc and hexagonal phases) and cobalt–nickel alloynanoparticles, J. Colloid Interface, 336 (2009) 814-819.

[28] D. Zhang, X. Ni, H. Zheng, Y. Li, X. Zhang, Z. Yang, Synthesis of needle-like nickel nanoparticles in water-in-oil microemulsion, Mater. Lett. 59 (2005) 2011-2014.

[29] Z. Ying, J. Shengming, Q. Guanzhou, Y. Min, Preparation of ultrafine nickel powder by polyol method and its oxidation product, Mater. Sci. Eng. B. 122 (2005) 222-225.

[30] K.J. Carroll, J.U. Reveles, M.D. Shultz, S.N. Khanna, E.E. Carpenter, Preparation of elemental Cu and Ni nanoparticlesby the polyol method: an experimental and theoretical approach, J. Phys. Chem. C. 115 (2011) 2656-2664.

[31] T. Hinotsu, B. Jeyadevan, C.N. Chinnasamy, K. Shinoda, K. Tohj, Size and structure control of magnetic nanoparticlesby using a modified polyol process, J. Appl. Phys. 95 (2004) 7477-7479.

[32] D. Li, S. Komarneni, Microwave-assisted polyol process for synthesis of Ni nanoparticles. J. Am. Ceram. Soc. 89 (2006) 1510-1517.

[33]. W. Xu, K.Y. Liew, H. Liu, T. Huang, C. Sun, Y. Zhao, Microwave-assisted synthesis of nickel nanoparticles, Mater. Lett. 62 (2008) 2571-2573.

[34] R. Abu-Much, A. Gedanken, Sonochemical synthesisunder a magnetic field: fabrication of nickel and cobaltparticles and variation of their physical properties, Chemistry 14 (2008) 10115-10122.

[35] S.L. Gafner, Y.Y. Gafner, Analysis of gas-phase condensation of nickel nanoparticles, J. Exp. Theor. Phys. 107 (2008) 712-722.

[36] H. Wang, X. Jiao, D. Chen, Monodispersed nickel nanoparticleswith tunable phase and size: synthesis, characterization, and magnetic properties, J. Phys. Chem. C. 112 (2008) 18793-18797.

[37] Y.L. Hou, S. Gao, Monodisperse nickel nanoparticles prepared from a monosurfactant system and their magnetic properties J. Mater. Chem. 13 (2003) 1510-1512.

[38] A. Kotoulas, M. Gjoka, K. Simeonidis, I. Tsiaoussis, M. Angelakeris, O. Kalogirou, C. Dendrinou-Samara, The role of synthetic parameters in the magnetic behaviour of relative large hcp Ni nanoparticles J. Nanopart. Res. 13 (2011) 1897-1908.

[39] E. Ramirez-Meneses, I. Betancourt, F. Morales, V. Montiel-Palma. C.C. Villanueva-Alvarado, M.E. Hernandez-Rojas, Superparamagnetic nickel nanoparticles obtained by anorganometallic approach, J. Nanopart. Res. 13 (2011) 365-374.

[40] G.G. Couto, J.J. Klein, W.H. Schreiner, D.H. Mosca, A.J.A. de Oliveira, A.J.G. Zarbin, Nickel nanoparticles obtained by a modified polyol process: synthesis, characterization, andmagnetic properties, J. Colloid. Interface. Sci. 311 (2007) 461-468.

[41] M.S. Hedge, D. Larcher, L. Dupont, B. Beaudoin, K. Tekaia- Elhsissen, J.M. Tarascon, Synthesis and chemical reactivity of polyol prepared monodisperse nickel powders, Solid State Ion 93 (1996) 33-50.

[42] K.S. Chou, K.C. Huang, Studies on the chemical synthesis of nanosized nickel powder and its stability, J. Nanopart. Res. 3 (2001) 127-132.

[43] Z. An, S. Pan, J. Zhang, Synthesis and Tunable Assembly of Spear-like Nickel Nanocrystallites: From Urchin-like Particles to Prickly Chains, J. Phys. Chem. C 113 (2009) 1346-1351.

[44] N.R. Roselina, A. Azizan, Z. Lockman, Synthesis of Nickel Nanoparticles via Non-Aqueous Polyol Method: Effect of Reaction Time, Sains Malays. 41 (2012) 1037-1042.

[45] P. Mukherjee, P.S. Roy, S.K. Bhattacharya, Improved carbonate formation from ethanol oxidation on nickel supported Pt–Rh electrode in alkaline medium at room temperature, Int. J. Hydrogen Energy 40 (2015) 13357-13367.

[46] P. Mukherjee, J. Bagchi, S. Dutta, The nickel supported platinum catalyst for anodic oxidation of ethanol in alkaline medium, S.K. Bhattacharya, Appl. Catal. A 506 (2015) 220-227.

[47] J.W. Park, E.H. Chae, S.H. Kim, Preparation of fine Ni powders from nickel hydrazine complex, Mater. Chem. Phys. 97 (2006) 371-378.

[48] D.P. Wang, D.B. Sun, H.Y. Yu, H.M. Meng, Morphology controllable synthesis of nickel nanopowders by chemical reduction process, J. Cryst. Growth 310 (2008) 1195-1201.

[49] L.H. Taller, A.H. Zimmerman, Nickel-hydrogen cycle testing. Review and analysis. El Segundo, California: The Aerospace Press; (2003)

[50] J.W. Park, E.H. Chae, S.H. Kim, Preparation of fine Ni powders from nickel hydrazine complex, Mater. Chem. Phys. 97 (2006) 371-378.

[51] D.P. Wang, D.B. Sun, H.Y. Yu, H.M. Meng, Morphology controllable synthesis of nickel nanopowders by chemical reduction process, J. Cryst. Growth 310 (2008) 1195-1201.

[52] D.V. Goia, Preparation and formation mechanisms of uniform metallic particles in homogeneous solutions, J. Mater. Chem. 14 (2004) 451-458.

[53] R.M.A. Tehrani, Ab.S. Ghani, The nanocrystalline nickel with catalytic properties on methanol oxidation in alkaline medium, Fuel Cells, 9 (2009) 579-587.

[54] M.P. Zach, R.M. Penner, Nanocrystalline nickel nanoparticles, Adv Mater. 12 (2000) 878-883.

[55] B. Habibi, R. Gahramanzadeh, Fabrication and characterization of non-platinum electrocatalyst for methanol oxidation in alkaline medium: Nickel nanoparticles modified carbon-ceramic electrode, Int. J. Hydrogen Energy 36 (2011) 1913-1923.

[56] M.A. Abdel Rahim, R.M. Abdel Hameed, M.W. Khalil, Nickel as a catalyst for the electro-oxidation of methanol in alkaline medium, J. Power Sources 134 (2004) 160-169.

[57] D. Takky, B. Beden, J.M. Leger, C. Lamy, Evidence for the effect of molecular structure on the electrochemical reactivity of alcohols: Part 1. Electrooxidation of the butanol isomers on noble metal electrodes in alkaline medium, J. Electroanal. Chem. 145 (1983) 461-466.

Highlights

- Ni nanoparticles of same average size are synthesized by modified polyol process.
- The maximum peak current density *Ip* (54.03 $mAmg^{-1}$) for BOR is obtained for Ni(4).
- *Ip* is 14 and 2.3 times more than bulk Pt and Pd electrodes respectively.
- The best electrode can also oxidise butanal and butanoate in addition to butanol.

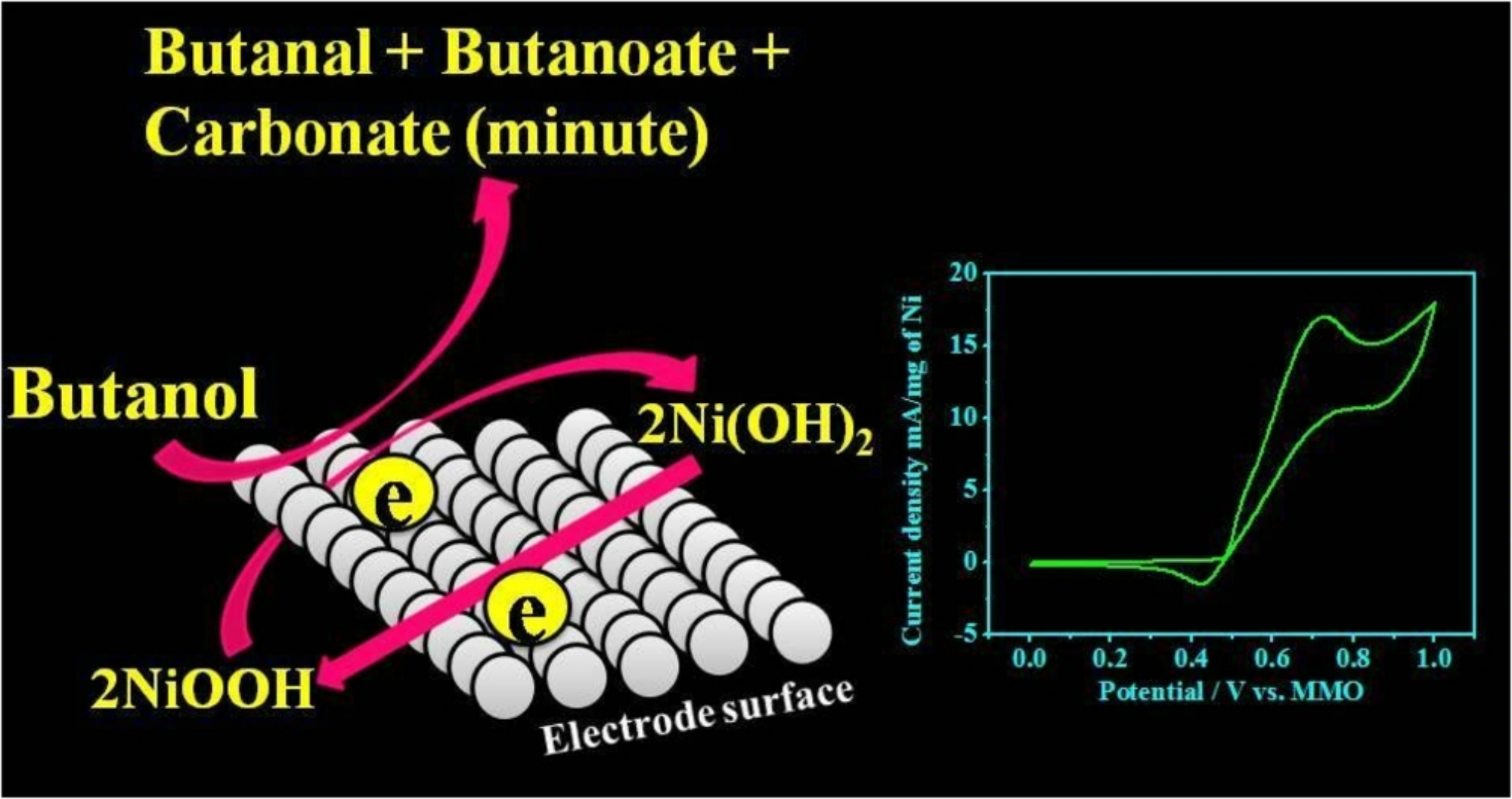
Butanal + Butanoate +
Carbonate (minute)
Butanol
2Ni(OH)2
e
e
2NiOOH
Electrode surface
Current density mA/mg of Ni
20
15
10
5
0
-5
0.0
0.2
0.4
0.6
0.8
1.0
Potential / V vs. MMO